J|A|C|S ARTICLES

Published on Web 07/02/2010

Multistage Collapse of a Bacterial Ribozyme Observed by Time-Resolved Small-Angle X-ray Scattering

Joon Ho Roh,*,†,‡,§ Liang Guo,|| J. Duncan Kilburn,‡ Robert M. Briber,*,† Thomas Irving,|| and Sarah A. Woodson*,‡

Department of Materials Science and Engineering, University of Maryland, College Park, Maryland 20742, T. C. Jenkins Department of Biophysics, Johns Hopkins University, Baltimore, Maryland 21218, NIST Center for Neutron Scattering Research, National Institute of Standards and Technology, Gaithersburg, Maryland 20899, and BioCAT, CSRRI and Department of BCPS, Illinois Institute of Technology, Chicago, Illinois 60616

Received May 6, 2010; E-mail: rohmio1973@gmail.com; rbriber@umd.edu; swoodson@jhu.edu

Abstract: Ribozymes must fold into compact, native structures to function properly in the cell. The first step in forming the RNA tertiary structure is the neutralization of the phosphate charge by cations, followed by collapse of the unfolded molecules into more compact structures. The specificity of the collapse transition determines the structures of the folding intermediates and the folding time to the native state. However, the forces that enable specific collapse in RNA are not understood. Using time-resolved SAXS, we report that upon addition of 5 mM Mg^{2+} to the *Azoarcus* group I ribozyme up to 80% of chains form compact structures in less than 1 ms. In 1 mM Mg^{2+}, the collapse transition produces extended structures that slowly approach the folded state, while $\geq$1.5 mM Mg^{2+} leads to an ensemble of random coils that fold with multistage kinetics. Increased flexibility of molecules in the intermediate ensemble correlates with a Mg^{2+}-dependent increase in the fast folding population and a previously unobserved crossover in the collapse kinetics. Partial denaturation of the unfolded RNA with urea also increases the fraction of chains following the fast-folding pathway. These results demonstrate that the preferred collapse mechanism depends on the extent of Mg^{2+}-dependent charge neutralization and that non-native interactions within the unfolded ensemble contribute to the heterogeneity of the ribozyme folding pathways at the very earliest stages of tertiary structure formation.

Introduction

Understanding the physical basis of events early in the folding process is crucial for mapping out the dynamics of RNAs. Unlike proteins, which fold in response to the hydrophobic effect, RNA folding is enabled by neutralization of the phosphate anionic charge by multivalent cations such as Mg^{2+}.[1,2] Charge neutralization triggers the formation of compact intermediates that are more flexible, with a shorter persistence length.[3] The compact intermediates subsequently undergo a further conformational search leading to the native state.[4,5]

A central question is how physical and chemical forces during counterion-induced collapse influence the outcomes of the folding process. Many conformational states are accessible at the beginning of the collapse transition from the unfolded state, and stochastic fluctuations among these cause individual molecules to fold along different paths.[6] The ensuing competition among parallel folding trajectories has been confirmed by many ensemble and single molecule experiments.[7,8] The observed folding kinetics and the fraction of RNA that reaches the native state in a biologically meaningful time depend on the specificity of the early transitions because different intermediate ensembles with different structures experience different energy barriers to folding.[9,10]

Previous studies of ribozyme folding suggest that neutralization of the phosphate charge by counterions results in nonspecific relaxation of the unfolded state, followed by sequence-specific folding to more compact and native-like structures.[11−16] In particular, small-angle X-ray scattering (SAXS) and footprinting studies of the *Tetrahymena* group I ribozyme showed that deletion of key tertiary interactions had no effect on the initial

† University of Maryland.
‡ Johns Hopkins University.
§ National Institute of Standards and Technology.
|| Illinois Institute of Technology.

(1) Draper, D. E. *RNA* **2004**, *10*, 335.
(2) Thirumalai, D.; Hyeon, C. *Biochemistry* **2005**, *44*, 4957.
(3) Caliskan, G.; Hyeon, C.; Perez-Salas, U.; Briber, R. M.; Woodson, S. A.; Thirumalai, D. *Phys. Rev. Lett.* **2005**, *95*, 4.
(4) Sosnick, T. R. *Protein Sci.* **2008**, *17*, 1308.
(5) Woodson, S. A. *Curr. Opin. Chem. Biol.* **2005**, *9*, 104.
(6) Thirumalai, D.; Lee, N.; Woodson, S. A.; Klimov, D. K. *Annu. Rev. Phys. Chem.* **2001**, *52*, 751.
(7) Zhuang, X. W. *Annu. Rev. Biophys. Biomol. Struct.* **2005**, *34*, 399.
(8) Li, P. T. X.; Vieregg, J.; Tinoco, I. *Annu. Rev. Biochem.* **2008**, *77*, 77.
(9) Russell, R.; Zhuang, X. W.; Babcock, H. P.; Millett, I. S.; Doniach, S.; Chu, S.; Herschlag, D. *Proc. Natl. Acad. Sci. U.S.A.* **2002**, *99*, 155.
(10) Thirumalai, D.; Woodson, S. A. *Acc. Chem. Res.* **1996**, *29*, 433.
(11) Das, R.; Travers, K. J.; Bai, Y.; Herschlag, D. *J. Am. Chem. Soc.* **2005**, *127*, 8272.
(12) Deras, M. L.; Brenowitz, M.; Ralston, C. Y.; Chance, M. R.; Woodson, S. A. *Biochemistry* **2000**, *39*, 10975.
(13) Fang, X. W.; Littrell, K.; Yang, X.; Henderson, S. J.; Siefert, S.; Thiyagarajan, P.; Pan, T.; Sosnick, T. R. *Biochemistry* **2000**, *39*, 11107.

 10.1021/ja103867p

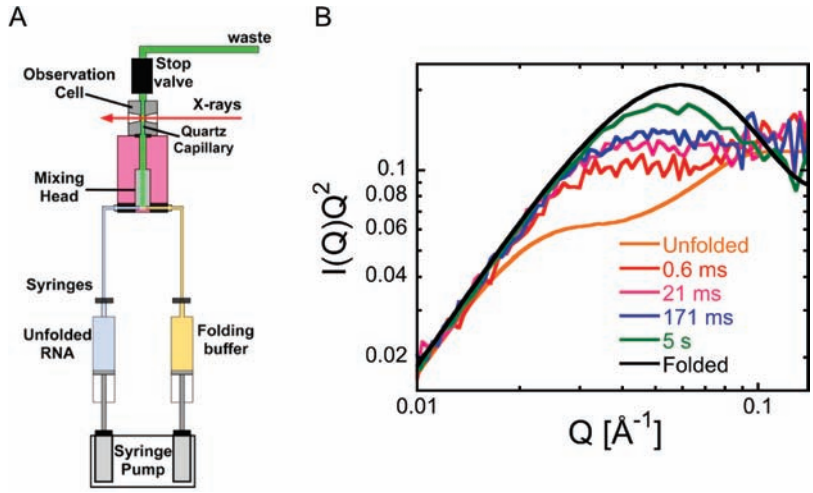

Figure 1. Time-resolved SAXS of *Azoarcus* ribozyme folding. (A) Schematic view of the stopped-flow mixer (SFM400). Syringes were loaded with unfolded RNA (1 mg/mL after mixing) in 20 mM Tris-HCl and folding buffer containing $MgCl_2$. The dead time (~0.6 ms) was minimized by a high flow rate and short distance from the small-volume mixer to the observation point. (B) Kratky plots of real-time folding data in 1.5 mM $MgCl_2$. Curve at 5 s (green) were in 5 mM $MgCl_2$. For time-resolved measurements (≤200 ms), 15−20 identical 1 ms data sets were averaged. Scattering data up to 5 s were acquired for 50 ms and averaged over 4 shots. For unfolded RNA in 20 mM Tris-HCl (orange) and folded RNA in 5 mM $MgCl_2$ (black) at equilibrium, data were collected for 1.6 s (4 times).

relaxation and contraction of the unfolded state ($\tau \sim 15$ ms).[14,17] However, these mutations blocked slow steps ($\tau \sim 0.1-100$ s) that reflect tertiary folding and reorganization of the misfolded ribozyme core.[18,19]

By contrast, the *Azoarcus* group I ribozyme and the catalytic domain of *Bacillus subtilis* RNase P experience a specific equilibrium collapse transition to native-like intermediates in the same Mg^{2+} concentration range as neutralization of the phosphate charge,[13,15,20] suggesting the native topology is established early in the folding process for these RNAs. Consistent with this hypothesis, these ribozymes refold rapidly under native conditions ($\tau = 5 - 50$ ms; 37 °C).[21−24] These observations support theoretical predictions that the yield of native RNA is highest when the collapse transition is specifically nucleated by a subset of native interactions.[6]

To determine whether counterion-induced collapse and nucleation of native-like structures can occur simultaneously in RNA, we studied the collapse transition kinetics of the *Azoarcus* group I ribozyme by stopped-flow SAXS. SAXS is well suited to studying the folding-driven structural changes because it provides information about the global structure, even when the conformations are dynamic or irregular.[25] Time-resolved SAXS using stopped-flow mixers or continuous-flow microfluidic chambers have been used to study the kinetics of protein folding[26,27] and RNA folding[14,17,28] and virus assembly.[29]

Taking advantage of a small volume mixer and fast X-ray detector, we show that the *Azoarcus* ribozyme exhibits multiple folding pathways with different kinetics and that partitioning between these pathways depends strongly on Mg^{2+} concentration. The rapid pathway has a collapse time less than 1 ms, similar to the estimated 1 ms collapse time of the RNase P catalytic domain[13,15,20] but at least 10 times shorter than previously reported for the *Tetrahymena* ribozyme.[14,17,30] More RNA partitions into the fast phase when the RNA interactions are partially denatured by urea, suggesting that the intrinsic heterogeneity of the unfolded ensemble underlies the various folding mechanisms and that phases slower than 1 ms arise from the rearrangement of non-native structures.[21]

Experimental Section

RNA Samples. The 195 nucleotide *Azoarcus* ribozyme was prepared by large-scale in vitro transcription of pAz-IVS DNA as previously described.[23,31] The RNA was concentrated (~10 mg/mL) and exchanged 3−4 times with 20 mM Tris-HCl (pH 7.5) using Centricon-30 concentrators (Amicon). The RNA samples were filtered through a 0.2 μm membrane (Millipore).

SAXS Measurements. Time-revolved SAXS experiments were performed with a Bio-Logic SFM-400 stopped-flow mixer (Figure 1A) coupled with a Pilatus 100K photon counting detector (Dectris) at BioCAT beamline 18-D at the Advanced Photon Source (Argonne National Laboratory). A 0.6 ms dead time was achieved

(14) Kwok, L. W.; Shcherbakova, I.; Lamb, J. S.; Park, H. Y.; Andresen, K.; Smith, H.; Brenowitz, M.; Pollack, L. *J. Mol. Biol.* **2006**, *355*, 282.
(15) Moghaddam, S.; Caliskan, G.; Chauhan, S.; Hyeon, C.; Briber, R. M.; Thirumalai, D.; Woodson, S. A. *J. Mol. Biol.* **2009**, *393*, 753.
(16) Pljevaljcic, G.; Klostermeier, D.; Millar, D. P. *Biochemistry* **2005**, *44*, 4870.
(17) Russell, R.; Millettt, I. S.; Tate, M. W.; Kwok, L. W.; Nakatani, B.; Gruner, S. M.; Mochrie, S. G. J.; Pande, V.; Doniach, S.; Herschlag, D.; Pollack, L. *Proc. Natl. Acad. Sci. U.S.A.* **2002**, *99*, 4266.
(18) Pan, J.; Woodson, S. A. *J. Mol. Biol.* **1998**, *280*, 597.
(19) Sclavi, B.; Sullivan, M.; Chance, M. R.; Brenowitz, M.; Woodson, S. A. *Science* **1998**, *279*, 1940.
(20) Fang, X. W.; Thiyagarajan, P.; Sosnick, T. R.; Pan, T. *Proc. Natl. Acad. Sci. U.S.A.* **2002**, *99*, 8518.
(21) Chauhan, S.; Behrouzi, R.; Rangan, P.; Woodson, S. A. *J. Mol. Biol.* **2009**, *386*, 1167.
(22) Chauhan, S.; Woodson, S. A. *J. Am. Chem. Soc.* **2008**, *130*, 1296.
(23) Rangan, P.; Masquida, B.; Westhof, E.; Woodson, S. A. *Proc. Natl. Acad. Sci. U.S.A.* **2003**, *100*, 1574.
(24) Fang, X. W.; Pan, T.; Sosnick, T. R. *Nat. Struct. Biol.* **1999**, *6*, 1091.
(25) Lipfert, J.; Doniach, S. *Annu. Rev. Biophys. Biomol. Struct.* **2007**, *36*, 307.
(26) Arai, M.; Ikura, T.; Semisotnov, G. V.; Kihara, H.; Amemiya, Y.; Kuwajima, K. *J. Mol. Biol.* **1998**, *275*, 149.
(27) Zhu, L.; Qin, Z. J.; Zhou, J. M.; Kihara, H. *Biochimie* **2004**, *86*, 127.
(28) Das, R.; Kwok, L. W.; Millett, I. S.; Bai, Y.; Mills, T. T.; Jacob, J.; Maskel, G. S.; Seifert, S.; Mochrie, S. G. J.; Thiyagarajan, P.; Doniach, S.; Pollack, L.; Herschlag, D. *J. Mol. Biol.* **2003**, *332*, 311.
(29) Canady, M. A.; Tsuruta, H.; Johnson, J. E. *J. Mol. Biol.* **2001**, *311*, 803.
(30) Schlatterer, J. C.; Kwok, L. W.; Lamb, J. S.; Park, H. Y.; Andresen, K.; Brenowitz, M.; Pollack, L. *J. Mol. Biol.* **2008**, *379*, 859.

by installing a microvolume mixer (MEC 22998, Bio-Logic) in the SFM and confirmed by time-resolved UV-absorption measurements (MOS-200) of the reduction of 2,6-dichlorophenolindophenol by ascorbic acid. The trigger for the stopped flow plungers was synchronized with the photon detector on the basis of the time-resolved X-ray absorption tests of a $ZnCl_2$ solution.

Folding experiments were carried out at 32 °C by mixing equal volumes of 2 mg/mL of unfolded RNA in 20 mM Tris-HCl and folding buffer containing 2X $MgCl_2$ in 20 mM Tris-HCl. The unfolded RNA was incubated for 5−10 min at 50 °C prior to the experiment, which we previously found minimizes misfolding and aggregation.[23] In some experiments, 3 M urea was added to the RNA and the folding buffer before mixing. Time-resolved scattering data were acquired for 1 ms intervals and read out in 4 ms. The high flux of the X-ray beam ($\sim 10^{13}$ photons per second) and the sensitivity of the detector provided a reasonable scattering profile over a Q range of 0.006−0.25 Å^{-1}, even with very short acquisition times. For each condition, 15−20 identical shots were averaged to obtain reasonable scattering statistics. Scattering data at folding intervals longer than 1 s were acquired for 50 ms and averaged over 4 shots. SAXS measurements of equilibrium titrations of 1 mg/mL of ribozyme with Mg^{2+} (Figure S1, Supporting Information) were carried out as previously described.[31]

SAXS Data Analysis. Following background subtraction, the scattering intensities, $I(Q)$, were converted into real-length pair distance distribution functions, $P(r)$, by indirect inverse Fourier transform using GNOM.[32] The radius of gyration, R_g, was obtained from the $P(r)$ representing the best fit to $I(Q)$ as previously described.[31] Fractional saturation of the folding transition, representing the amount of remaining unfolded RNA, Φ_U, was estimated from $R_g^2 = \Phi_U R_{g,U}^2 + (1 - \Phi_U)R_{g,F}^2$, in which $R_{g,U}$ (unfolded) and $R_{g,F}$ (folded) are obtained from RNAs equilibrated for 30 min in 0 and 10 mM $MgCl_2$.

Results

Rapid Collapse of the *Azoarcus* Ribozyme in Mg^{2+}. The collapse transition under equilibrium conditions produces a large change in the scattering curve of the *Azoarcus* ribozyme, reflecting a decrease in R_g from 60 Å for the unfolded RNA in no $MgCl_2$ to 31 Å for the folded RNA in 5 mM $MgCl_2$ (Figure S1, Supporting Information).[31] In the range of 0.5−2 mM $MgCl_2$, the *Azoarcus* ribozyme forms an intermediate (I_C) that is as compact as the native state and contains the core helices and some tertiary interactions.[23,31,33] At 32 °C in 1 mg/mL of RNA, the midpoint for the transition to I_C is 0.88 mM $MgCl_2$ (Figure S1, Supporting Information), which is 40% less than the 1.5 mM Mg^{2+} needed to equal the number of charges on the phosphates (3 mM).

We used stopped-flow SAXS to follow the collapse process in real time (Figure 1A and Experimental Section). Unfolded RNA in 20 mM Tris-HCl and $MgCl_2$ solution were mixed with a dead time of 0.6 ms, and data were acquired for 1 ms every 5 ms, starting at 0.6 ms and continuing to 200 ms. Scattering data were also acquired in 5 mM $MgCl_2$ at folding times up to 10 min.

The rapid compaction of the RNA with folding time can be seen in Kratky plots of the scattering intensity (Figure 1B). The Kratky plot of the unfolded ribozyme increases over the intermediate Q range 0.04−0.1 Å^{-1} (Figure 1B and Figure S2, Supporting Information), reflecting the predominantly extended conformations characteristic of the unfolded RNA at low ionic strength. After only 0.6 ms folding time in 1.5 mM Mg^{2+}, a plateau in the intermediate Q region reveals evidence of a collapse transition in the submillisecond time scale. After 21 ms, a plateau in the Kratky plot is consistent with random coil-like structures.[34] As expected, the Kratky plot of the folded RNA exhibits a maximum at $Q = 0.06$ Å^{-1}, reflecting a relatively homogeneous and compact structure (Figure 1B).

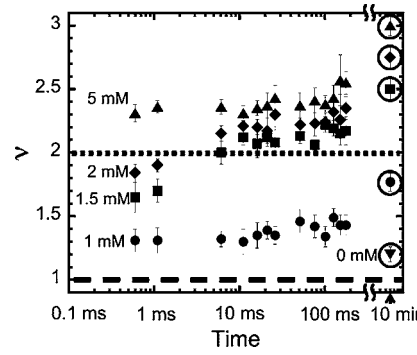

Figure 2. Structure of early folding ensembles in Mg^{2+}. Time-dependent exponents, ν, in different $MgCl_2$ were determined from linear fits to $\log[I(Q) \sim Q^{-\nu}]$ vs $\log Q$ for $0.05 < Q < 0.1$ Å^{-1} (see Figure S3, Supporting Information). Error bars are from the statistics of the fit. Dashed line corresponds to the worm-like chain ($\nu = 1$). Dotted line corresponds to the random coil-like chain ($\nu = 2$). For an ideal sphere, $\nu = 4$. The circled symbols represent ν values at equilibrium.

As the Mg^{2+} concentration in the folding reaction is raised from 1 to 5 mM, the RNA becomes progressively more compact within the first millisecond of the folding reaction (Figure S2A, Supporting Information). In 1 mM Mg^{2+}, which is near the midpoint of the equilibrium folding curve, the lack of a defined peak in the Kratky plots at 11 and 51 ms indicates the system contains a mixture of disordered structures. In contrast, the early intermediates in 2 and 5 mM Mg^{2+} are much more compact. This difference is even greater at 171 ms, at which point the Kratky plot of RNA refolded in 5 mM Mg^{2+} displays a well-developed peak at $Q \sim 0.04$ Å^{-1} (Figure S2D, Supporting Information). In general, the changes in the scattering curves indicate that local interactions measured at wide scattering angles ($Q \sim 0.1$ Å^{-1}) and the global fold measured at narrow scattering angles ($Q < 0.05$ Å^{-1}) form on the same time scales for this ribozyme.

Structure of Early Folding Intermediates. The average flexibility and extension of the RNA chains following initial collapse was analyzed by comparing the exponent, ν, for $I \sim Q^{-\nu}$ over the range 0.05 Å$^{-1} < Q < 0.1$ Å^{-1} (Figure 2 and Figure S3, Supporting Information). This region of the scattering curves is more sensitive to the orientations of neighboring segments in the RNA than the Guinier region, $Q < 0.05$ Å^{-1}, which reports the global shape. The value of $\nu \sim 1.2$ of the unfolded RNA is characteristic of rigid wormlike polymers (Figure 2), in agreement with our previous result that the unfolded RNA has an extended structure ($l_P \approx 21$ Å) at low ionic strength.[3] For the fully folded ribozyme, $\nu = 3$ (Figure 2), consistent with a collapsed chain ($l_P \approx 10$ Å).

The ν values as a function of folding time are plotted in Figure 2 for each Mg^{2+} concentration. When the ribozyme was folded in 1 mM Mg^{2+}, the RNA chains remain extended ($\nu = 1.3-1.5$ at 170 ms and 1.75 at 10 min) compared with a random coil ($\nu \sim 2$), perhaps due to incomplete neutralization of the phosphate

(31) Chauhan, S.; Caliskan, G.; Briber, R. M.; Perez-Salas, U.; Rangan, P.; Thirumalai, D.; Woodson, S. A. *J. Mol. Biol.* **2005**, *353*, 1199.
(32) Semenyuk, A. V.; Svergun, D. I. *J. Appl. Crystallogr.* **1991**, *24*, 537.
(33) Perez-Salas, U. A.; Rangan, P.; Krueger, S.; Briber, R. M.; Thirumalai, D.; Woodson, S. A. *Biochemistry* **2004**, *43*, 1746.
(34) Roe, R. *Methods of X-ray and Neutron Scattering in Polymer Science*; Roe, R., Ed.; Oxford University Press: New York, 2000;p 155.

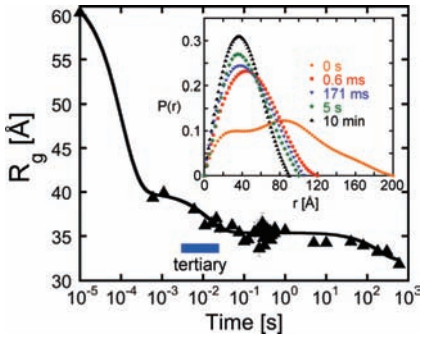

Figure 3. Multistage collapse kinetics. Decrease in R_g over time from the unfolded state (60.5 Å) to the folded state (31 Å) during refolding in 5 mM $MgCl_2$. Error bars represent the uncertainty in R_g from the data inversion. Solid line is the best fit to a triple exponential decay function ($\tau_1 \leq 0.2$ ms, $\tau_2 = 20$ ms, $\tau_3 = 170$ s; see Table S1, Supporting Information). Blue bar, 5−20 ms time window in which tertiary interactions are detected by hydroxyl radical footprinting.[22] Inset: Pair distance distribution function, $P(r)$, for RNA folding in 5 mM $MgCl_2$ at the times shown.

charges in 1 mM Mg^{2+}. Above 1 mM Mg^{2+}, the RNA population after 0.6 ms of folding became increasingly flexible and compact, with ν values rising to 1.65 for 1.5 mM Mg^{2+}, 1.85 for 2 mM Mg^{2+}, and 2.3 for 5 mM Mg^{2+} (Figure 2 and Figure S2, Supporting Information). Thus, when there are a sufficient number of counterions, a random-coil state is achieved rapidly.

From these results, we conclude that the chain flexibility and the degree of compaction in the first few milliseconds of folding are remarkably sensitive to the association of Mg^{2+} ions with the RNA. A comparison of the right and left sides of Figure 2 shows that the early collapse transition (and thus the folding kinetics) is more sensitive to Mg^{2+} than the stability of the native state. When reactions in 1.5 mM and 5 mM $MgCl_2$ are compared, values of ν differ by 0.65 at 0.6 ms but only by 0.4 at 171 ms and 0.5 at 10 min.

Partitioning of Multiphase Folding Kinetics. To examine the kinetic pathways for collapse and tertiary folding, the progress of the folding reaction was determined from the $P(r)$ and R_g for each Mg^{2+} concentration. Distance distribution functions, $P(r)$, obtained from the indirect inverse Fourier transform of $I(Q)$ were consistent with the formation of more globular structures over time (Figure 3 inset) and revealed a sharp decrease in R_g, within the first 0.6 ms of folding (Figure 3). These data show that most of the ribozyme population has collapsed into compact structures by 1 ms in 5 mM $MgCl_2$.

In addition to the submillisecond collapse that accounts for most of the decrease in R_g, we also observed an additional fast transition around 20 ms and a very slow transition between 100 and 300 s. The multiphase folding kinetics measured by stopped-flow SAXS was qualitatively similar to observations from stopped-flow fluorescence and hydroxyl radical footprinting at 37 °C.[21] Thus, folding of the *Azoarcus* ribozyme involves at least three kinetic phases and stretches over time scales from $\leq 10^{-3}$ to $\sim 10^{3}$ s.

Partitioning of the RNA population among different folding processes was evaluated by linking the folding kinetics to the thermodynamic stability of the folded RNA. We previously showed that the change in X-ray scattering by the *Azoarcus* ribozyme with increasing Mg^{2+} concentration can be described by an equilibrium between unfolded and compact states of the RNA.[15,31] We used this two-state model to obtain the average fraction of unfolded chains, $\Phi_U(t)$, at each folding time (Figure

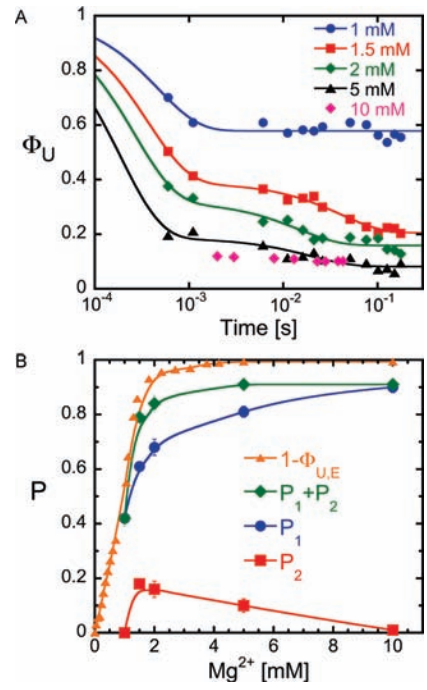

Figure 4. Mg^{2+} determines partitioning of collapse kinetics. (A) Fraction of unfolded *Azoarcus* ribozyme, $\Phi_U(t)$, refolded in 1, 1.5, 2, 5, and 10 mM $MgCl_2$. Solid lines represent the best fit to eq 1; fit parameters are in Table S1, Supporting Information. See Figure S4A,B (Supporting Information) for further data. (B) Partitioning of RNA population into burst (P_1; blue) and second phase (P_2; red) within 200 ms. 1-$\Phi_{U,E}$ is the fraction of folded RNA at equilibrium. The difference between 1-$\Phi_{U,E}$ (orange) and $P_1 + P_2$ (green) represents long-lived misfolded RNAs. Error bars are from the uncertainty of fits in (A).

S1, Supporting Information; Experimental Section). The decrease in $\Phi_U(t)$ over the first 200 ms was fit to a double exponential decay function

$$\Phi_U(t) = 1 - P_1(1 - \exp(-t/\tau_1)) - P_2(1 - \exp(-t/\tau_2)) \quad (1)$$

in which τ_1 and τ_2 are the time constants associated with the initial collapse and the second transition, and P_1 and P_2 are their partition coefficients, respectively.

As seen above from the change in ν (Figure 2), the extent of collapse in the first 0.6 ms rose significantly as the Mg^{2+} concentration in the folding reaction was increased (Figure 4A). In 1 mM Mg^{2+}, the initial stage of collapse (P_1) accounted for 30% of the RNA population within 0.6 ms, while in 10 mM Mg^{2+}, the *Azoarcus* ribozyme was 90% folded in this time (Figure 4B). Although the native structure is fully stable above 5 mM $MgCl_2$, 10% of the RNA remained unfolded after 200 ms (Figure 4B). This presumably reflects RNA chains that are kinetically trapped in misfolded states.[21]

The second process, with $\tau_2 = 20-40$ ms, accounted for another 18% of the unfolded fraction (Figure 4B). Its appearance in 1.5−2 mM Mg^{2+} correlated with the crossover to random coil behavior ($\nu = 2$; Figure 2), suggesting that it represents a process that is only populated when the chains are able to explore compact configurations. As the RNA tertiary interactions became fully stable in 5 mM Mg^{2+}, the amplitude of the second phase decreased and finally vanished from the observation window.

Choice of Folding Pathways Linked to the Structure of the Unfolded State. Multistage collapse is thought to arise from partitioning of the RNA population into parallel folding

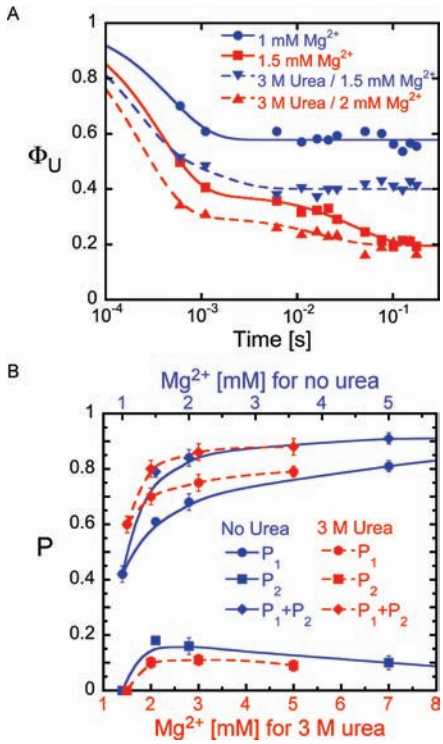

Figure 5. Urea increases the fraction of rapidly compacting RNA. Time-dependent folding of 3 M urea-relaxed ribozyme compared with urea-free ribozyme. (A) Fraction of unfolded *Azoarcus* ribozyme as in Figure 4A. Solid lines, no urea; dashed lines, with 3 M urea. Colors denote conditions of isostability determined from equilibrium titrations (Figure S1, Supporting Information). See Figure S4C (Supporting Information) for further data. (B) Partition factors for the first two phases (P_1 and P_2) with urea (red) and without urea (blue). The Mg^{2+} concentration axis for urea-free reactions (top) is shifted by a factor of 1.4 relative to the lower *x* axis.

trajectories, some of which involve kinetically trapped intermediates.[10] Alternatively, the kinetic phases might represent sequential steps between stable intermediates.[9,14] To determine whether competition from non-native interactions impedes early folding steps of the *Azoarcus* group I ribozyme, we examined the effect of urea on the collapse kinetics.

Urea was expected to smooth out the free-energy landscape of the unfolded RNA ensemble, which contains some secondary structure.[23] In agreement with the idea that urea destabilizes interactions in the unfolded state, the R_g of the unfolded ribozyme was 67.5 Å in 3 M urea, 7 Å larger than the unfolded RNA without urea (Figure S1, inset, Supporting Information). The midpoint of the folding equilibrium shifted to 1.24 mM Mg^{2+} in 3 M urea, which was 1.4 times higher than without urea (Figure S1, Supporting Information). Because urea did not change the cooperativity of the folding transition ($n = 2.3$), its destabilizing effect on the tertiary structure could be compensated by raising the Mg^{2+} concentration 1.4-fold.

Preincubation of the unfolded RNA in urea increased the fraction of fast-collapsing RNA about 50%, compared to isostable urea-free reactions (Figure 5). Thus, urea not only accelerates remodeling of misfolded RNAs in the late stages of folding but also perturbs the initial collapse process. Urea also increased the rate of the second process slightly (Table S1, Supporting Information). These results suggested that the slower P_2 phase arose from partitioning into ensembles that experience higher energy barriers along the folding trajectory, presumably due to interference from non-native interactions. If the kinetic phases represented sequential folding, we would have expected urea to increase the folding times without changing the amplitudes of each phase. Even in 3 M urea, about 10% of the RNA population requires more than a minute to fold (Figure 5B).

Discussion

RNA folding pathways are often heterogeneous, spanning many time scales and involving native and non-native intermediates.[2,4] This heterogeneity can arise very early in the folding process due to stable local interactions in the unfolded RNA ensemble.[35,36] The specificity of the folding trajectories influences RNA self-assembly, ligand recognition, and regulation, yet the physical forces driving the nucleation and collapse of RNA tertiary structure are poorly understood.

Our time-resolved SAXS results show that the *Azoarcus* ribozyme forms compact structures in less than a millisecond under native conditions, about 10-fold faster than the earliest reported transitions of the *Tetrahymena* ribozyme.[14,17,30] The structures formed within this time window are compact, consistent with specific folding of the RNA. Importantly, partitioning of the *Azoarcus* ribozyme among different collapse processes depends critically on the Mg^{2+} concentration. Below, we discuss how electrostatic interactions determine the topology of the RNA chains at an early stage of the folding process and the search for native-like conformations.

Our SAXS, fluorescence, and footprinting results are all consistent with the early formation of native structure and suggest that the time scales for collapse and tertiary folding overlap in this RNA (blue bar; Figure 3). We observe at least three different time-dependent processes by stopped-flow SAXS, with time constants $\tau_1 \leq 1$ ms, $\tau_2 = 20-40$ ms, and $\tau_3 \approx 170$ s. These global structural changes agree well with earlier stopped-flow fluorescence and kinetic hydroxyl radical footprinting results probing the formation of local tertiary interactions, after accounting for differences in temperature and Mg^{2+} concentration.[21,22] In 15 mM Mg^{2+}, footprinting showed that tertiary interactions form throughout the wild-type ribozyme within 5−20 ms at 37 °C.[22] Two fast transitions were also detected by stopped-flow fluorescence ($\tau_1 \leq 10$ ms and $\tau_2 = 30$ ms) and were assigned to formation of the native-like I_C intermediate and the folded state, respectively.[21]

Previous biochemical experiments also showed that 5−15% of the *Azoarcus* ribozyme population folded through slow pathways (1 and 100 s at 37 °C) that involve reorganization of interactions near the central triple helix and the P3/P7 pseudoknot.[21] Refolding of such misfolded intermediates explains the very slow transitions ($\tau_3 \sim 170$ s) observed here.

The heterogeneity of the collapse kinetics in the *Azoarcus* ribozyme can be explained by partitioning of the RNA population into the parallel folding pathways (Figure 6). This partitioning model is supported by footprinting and nondenaturing gel electrophoresis experiments showing that most of the RNA forms all of the tertiary contacts in 5−20 ms, yet a small amount of RNA remains unfolded up to 5 min.[21] This model implies that the structural collapse probed by scattering profiles mostly reflects the native-like intermediates, and the various kinetic phases represent subpopulations (U^1, U^2, U^3) that fold through different transition states (Figure 6).

(35) Ditzler, M. A.; Rueda, D.; Mo, J. J.; Hakansson, K.; Walter, N. G. *Nucleic Acids Res.* **2008**, *36*, 7088.
(36) Heilman-Miller, S. L.; Woodson, S. A. *J. Mol. Biol.* **2003**, *328*, 385.

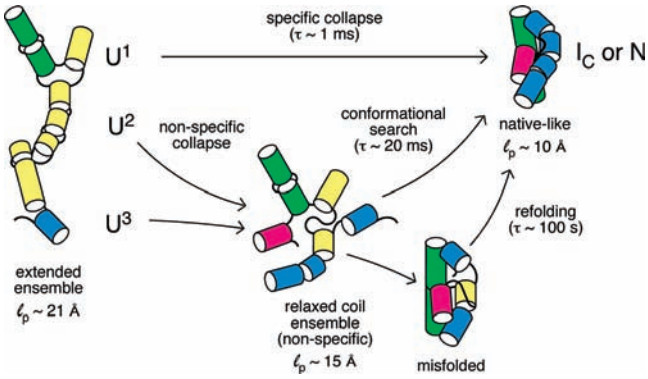

Figure 6. Folding nucleation and collapse of the *Azoarcus* ribozyme. Parallel folding from subpopulations of the unfolded state, U^1, U^2, and U^3, leads to heterogeneous folding kinetics. Direct folding to the native state (U^1) is favored by higher Mg^{2+} concentration or by partially denaturing amounts of urea. U^2 is populated only when Mg^{2+} concentration is higher than the midpoint of the equilibrium folding transition (0.88 mM) and has a cusp at 1.5−2 mM Mg^{2+}. Left and middle cartoons represent hypothetical structures in the unfolded and non-native relaxed coil ensembles. Average persistence lengths (l_p) are from fits to $P(r)$ as previously described.[3]

This picture is remarkably consistent with theoretical predictions that folding proceeds rapidly to the native state when the collapse transition is nucleated by specific native interactions.[6,37] When a protein or RNA is driven into compact structures before it has the opportunity to search out the correct topology, the initial collapse transition becomes nonspecific, producing structures that are mostly non-native. Theoretical models suggest that nonspecific collapse is followed by a diffusive search across low-energy barriers for more compact structures, and subsequently, by activated transitions from metastable misfolded states.[6] The smoothness of the free energy landscape determines the extent to which individual molecules fold along different paths and the barriers to folding.[10,38]

Accordingly, we postulate that the fastest collapse transitions in our experiments represent molecules (U^1) that fold directly to the native structure, while the second phase ($\tau_2 \sim 20$ ms) represents a subpopulation (U^2) in which the initial collapse is nonspecific. The ensuing search for stably folded and native-like structures is impeded by incorrect local contacts. The slowest phase represents the small population (U^3) that becomes trapped in long-lived misfolded structures. Since urea increased the size of the initial burst (P_1) and reduced partitioning into the second phase (P_2), the ensemble of initial structures is a critical factor driving the population of the folding landscape and the flux through discrete folding pathways. A similar effect was observed in the *Tetrahymena* ribozyme, that folds slowly in Mg^{2+} from an unfolded state in low ionic strength but exhibits a higher flux through fast folding pathways when the RNA is prestructured in Na^+.[9,39,40]

An alternative explanation for multiphasic collapse kinetics is stepwise folding through a series of intermediate states. This model, however, cannot explain why urea increased the folding rate (τ_2) and changed the partition coefficients P_1 and P_2. In addition, the plateaus in the SAXS progress curves at $R_g = 35$ and 40 Å are inconsistent with scattering from pure populations of known equilibrium folding intermediates ($R_g = 33$ and ~55 Å).[21,31] By the time the plateaus in the kinetic experiments are reached, our footprinting and fluorescence results show that some of the population has already folded completely. Overall, the data are better explained by parallel folding trajectories (Figure 6) than by sequential folding.

A major conclusion from our results is that the partitioning among different folding pathways depends on interactions of the RNA with counterions. First, we observe that Mg^{2+} increases the fraction of chains that form compact structures within 1 ms. Mg^{2+} may favor specific nucleation of the correct fold by stabilizing long-range tertiary interactions[22] or simply by reducing the RNA persistence length. Second, the non-native collapse ($\tau_2 = 20$ ms) emerges in Mg^{2+} concentrations above the midpoint of the equilibrium titration (0.88 mM Mg^{2+}) and maximizes near 1.5 mM Mg^{2+}, in which electrostatic neutralization is complete. Flux through this pathway correlates with the crossover from extended intermediates in 1 mM Mg^{2+} to random-coil configurations in 2 mM Mg^{2+}. Mg^{2+} has the same effect on the folding kinetics when the unfolded RNA is partially denatured with urea (Figure 5B).

We propose that Mg^{2+} concentrations sufficient to fully stabilize the folded RNA (≥1.5 mM) allow the RNA to form compact structures in the absence of specific long-range interactions, resulting in a subpopulation that must search for a stable fold after collapse has occurred.[6] Whether this effect requires multivalent counterions remains to be determined. Urea favors the specific collapse pathway by relaxing non-native interactions that may be present in the unfolded ensemble and by increasing the number of energetically favorable contacts needed to drive a chain through the collapse transition. Urea also lowers the energetic barrier of the conformational search in the second phase by destabilizing incorrect structures. These effects of urea occur early during folding and are distinct from the previously documented ability of denaturants to accelerate slow refolding transitions by raising the free energy of metastable misfolded states.[41,42]

In contrast to the *Azoarcus* ribozyme, the *Tetrahymena* ribozyme predominantly folds through misfolded intermediates.[41] To assess whether this difference can be discerned from the collapse kinetics, we compared the Kratky plots for the two RNAs in 5 mM Mg^{2+}. The scattering profile of the *Azoarcus* ribozyme after 0.6 ms of folding (Figure S1A, Supporting Information) contained a more pronounced peak than reported for the *Tetrahymena* ribozyme after 7 ms of folding time and is more comparable with the *Tetrahymena* ribozyme after 44 ms.[17] Not only does the *Azoarcus* ribozyme collapse and fold about than 10 times faster than the *Tetrahymena* ribozyme (in the first two phases) but also the initial collapsed population (or fractional weight) is about two times larger for the *Azoarcus* ribozyme than for the *Tetrahymena* ribozyme. Thus, the overall time needed to form compact structures in the population and the heterogeneity of the collapse kinetics correlates with the propensity of each ribozyme to partition into native structures instead of non-native structures.

Conclusion

Our time-resolved structural studies demonstrate that native-like conformations of the *Azoarcus* ribozyme form within the same time window as the initial collapse transition in Mg^{2+} but that the

(37) Guo, Z. Y.; Thirumalai, D. *Biopolymers* **1995**, *36*, 83.
(38) Socci, N. D.; Onuchic, J. N.; Wolynes, P. G. *Proteins* **1998**, *32*, 136.
(39) Shcherbakova, I.; Gupta, S.; Chance, M. R.; Brenowitz, M. *J. Mol. Biol.* **2004**, *342*, 1431.
(40) Heilman-Miller, S. L.; Pan, J.; Thirumalai, D.; Woodson, S. A. *J. Mol. Biol.* **2001**, *309*, 57.
(41) Pan, J.; Thirumalai, D.; Woodson, S. A. *J. Mol. Biol.* **1997**, *273*, 7.
(42) Pan, T.; Fang, X.; Sosnick, T. *J. Mol. Biol.* **1999**, *286*, 721.

heterogeneity of the folding kinetics depends strongly on the presence of counterions and the average compactness (or flexibility) of the polynucleotide chain. Our results are best explained by subpopulations that fold either through rapid and direct nucleation of the tertiary interactions, nonspecific collapse followed by short-range structural rearrangements, or refolding of long-lived, misfolded structures. The folding landscape can be smoothed by destabilizing interactions in the unfolded state; however, partitioning among these paths is still influenced by Mg^{2+} concentration. These observations demonstrate the importance of electrostatic interactions for the nucleation of long-range tertiary structure in RNA.

Acknowledgment. The authors thank D. Thirumalai for stimulating discussion, R. Behrouzi for preparation of RNA samples, and M. Mayerle for preparation of T7 RNA polymerase. This work was supported by NIST and the NIH (GM60819 to S.W.). Use of the Advanced Photon Source was supported by the U.S. Department of Energy, Basic Energy Sciences, Office of Science, under contract No. W-31-109-ENG-38. BioCAT is a National Institutes of Health-supported Research Center RR-08630.

Supporting Information Available: Time constants, equilibrium titration results, Kratky plots, and further time-resolved SAXS data. This material is available free of charge via the Internet at http://pubs.acs.org.

JA103867P